[7]Spence, D. A., "The Lift on a Thin Aerofoil with a Blown Flap," RAE TN Aero 2450, May 1956, Royal Aircraft Establishment, Farnborough, England.

[8]Herold, A. C., "A Two-Dimensional, Interative Solution for the Jet Flap," CR-2190, Feb. 1973, NASA.

[9]Dvorak, F. A., "Calculation of Turbulent Boundary Layers and Wall Jets over Curved Surfaces," *AIAA Journal*, Vol. 11, No. 4, April 1973, pp. 517-524.

[10]Goradia, S. H. and Colwell, G. T., "Parametric Study of a Two-Dimensional Turbulent Wall Jet in a Moving Stream with Arbitrary Pressure Gradient," *AIAA Journal*, Vol. 9, No. 11, Nov. 1971, pp. 2156-2165.

[11]Kacker, S. C. and Whitelaw, J. H., "Some Properties of the Two-Dimensional Turbulent Wall Jet in a Moving Stream," *Journal of Applied Mechanics*, Vol. 35, No. 4, Dec. 1968, pp. 641-651.

[12]Schlichting, H., *Boundary Layer Theory*, McGraw-Hill, New York, 1968, pp. 590-609.

[13]Bangert, L. H., "The Turbulent Wall Jet with an Initial Boundary Layer," AIAA Paper 71-612, Palo Alto, Calif., 1971.

[14]Gartshore, I. S. and Newman, B. C., "The Turbulent Wall Jet in an Arbitrary Pressure Gradient," *The Aeronautical Quarterly*, Vol. XX, Pt. I, Feb. 1969, pp. 25-56.

[15]Coles, D., *Proceedings, Computation of Turbulent Boundary Layers—1968, AFOSP-IFP-Stanford Conference*, Vol. II, Aug. 18-25, 1968, pp. 1-46.

[16]Lawford, J. A. and Foster, D. N., "Low Speed Wind Tunnel Tests on a Wing Section with Plain Leading- and Trailing-Edge Flaps Having Boundary Layer Control by Blowing," RAE TR 69078, April 1969, Royal Aircraft Establishment, Farnborough, England.

JANUARY 1975 J. AIRCRAFT VOL. 12, NO. 1

Thin-Airfoil Theory of an Ejector-Flapped Wing Section

Henry W. Woolard*
U.S. Air Force Flight Dynamics Laboratory, Wright-Patterson Air Force Base, Ohio

A theoretical analysis of the aerodynamics of a thin ejector-flapped wing section (augmentor wing) is presented. The idealized external and internal (ejector) flowfields and their approximate interfacing are treated. The linearized external flowfield analysis is an extension of Spence's method for jet-flapped airfoils. Summary curves of the section lift and pitching-moment characteristics and their relation to the ejector characteristics are presented. Fourier coefficients are tabulated for use in calculating airfoil surface pressure distributions and other flowfield details. The idealized lift performance of an ejector-flapped wing relative to a jet augmented flapped wing is compared and the ejector-flapped wing is found to be substantially superior at low forward-speed ratios. The relation of the present work to that of Y. Y. Chan is noted.

Nomenclature

A = cross-sectional area
b_f = ejector-flap span
c = airfoil chord ($c = 1$ in external aerodynamics analysis)
c_f = flap chord
c_h = flap hinge-moment coefficient about flap leading edge, based on c_f^2 (positive, trailing-edge down)
c_j = primary-jet installed momentum coefficient, $\rho U_j^2 \bar{h}_j / q_\infty c$
$\hat{c}_j$ = primary-jet uninstalled momentum coefficient, $\rho \hat{U}_j^2 h_j / q_\infty c$
c_j^* = primary-jet test momentum coefficient, $\rho U_j h_j \hat{U}_j / q_\infty c$
c_J = ejector exit-flow momentum coefficient, $\rho U_E^2 h_E / q_\infty c$
c_l = lift coefficient
c_{m_0} = airfoil nose-up pitching-moment coefficient about the leading edge
c_{nf} = flap normal-force coefficient
c_p = pressure coefficient, $(p - p_\infty)/q_\infty$; for small perturbations, $-2u'/U_\infty$
c_Q = thin-airfoil suction coefficient, $Q/U_\infty c$
c_Q = ejector net suction coefficient, $(U_s - U_\infty) h_s / U_\infty c$
$\check{c}_Q$ = ejector gross suction coefficient, $U_s h_s / U_\infty c$; $(\check{c}_Q = c_Q + \bar{h}_s/c)$
c_T = ejection net-thrust coefficient, $(\rho U_E^2 h_E - \rho U_s U_\infty h_s / q_\infty c$
$\hat{c}_t$ = primary-jet uninstalled net thrust coefficient, $\rho \hat{U}_j (\hat{U}_j - U_\infty) h_j / q_\infty c$
E_n = Fourier coefficients for trailing jet-sheet vorticity distribution
$f(x)$ = nondimensional vorticity distribution along the airfoil, $f(x) = \gamma(x)/U_\infty c$
$g'(x)$ = nondimensional vorticity distribution along the trailing jet sheet, $g'(x) = \gamma(x)/U_\infty c$
h_e, h_E = heights at ejector diffuser inlet and exit, respectively
$\bar{h}_j$ = mean height of ejector primary-jet nozzle, A_j/b_f
h_s = mean height of ejector secondary flow passage at primary-jet, A_s/b_f
p = static pressure
P = total pressure
q_∞ = freestream dynamic pressure, $(\rho/2) U_\infty^2$
Q = two-dimensional ideal flow sink strength
u = local velocity parallel to freestream
u' = perturbation velocity, $(u - U_\infty)$
U = mean local axial velocity within the ejector (except U_∞)
$\hat{U}_j$ = primary-jet uninstalled isentropic velocity, $[(2/\rho)(P_j - p_\infty)]^{1/2}$
$\tilde{U}_x$ = $U_x/\hat{U}_j$, where $x = j, s, E$, etc.
U_∞ = freestream velocity
$\tilde{U}_\infty$ = forward-speed parameter, $U_\infty/\hat{U}_j$
w = downwash velocity, positive downward
x, y = rectangular coordinates, see Fig. 2
x_s = chordwise location of sink on airfoil of unit chord
X = $[1 - (1 - x)^{1/2}]/[1 + (1 - x)^{1/2}]$
α = angle of attack
γ = vorticity, $d\Gamma/dx$ or $(u'_u - u'_l)$
Γ = total circulation
δ_f = trailing-edge flap deflection angle, positive for trailing-edge down
ϵ = local slope of airfoil surface
θ, φ = polar coordinates defined by Eq. (27)
λ = $4/c_J$
ξ, η = dummy variables
ρ = density
σ = $\sigma = 1$ for an upper-surface sink, $\sigma = -1$ for a lower-surface sink
Ω_D = ejector diffuser area ratio, A_E/A_e

Subscripts and Superscripts

Ω_j = ejector injection area ratio, A_s/A_j
a = denotes the airfoil
J = denotes the trailing jet sheet
T = denotes the trailing streamline for an unblown airfoil
$'$ = denotes differentiation with respect to the indicated argument (except u')
D = denotes the diffuser
e = ejector station e, see Fig. 6

Presented as Paper 74-187 at the AIAA 12th Aerospace Sciences Meeting, Washington, D.C., January 30-February 1, 1974; submitted February 12, 1974; revision received July 22, 1974.

Index categories: Aircraft Aerodynamics (including Component Aerodynamics); Subsonic and Transonic Flow; Jets, Wakes, and Viscid-Inviscid Flow Interactions.

*Aerospace Engineer, Flight Control Division, Control Criteria Branch (FGC). Associate Fellow AIAA.

E = ejector station E, see Fig. 6
EF = denotes an ejector-flapped wing
f = denotes the trailing-edge flap
j = denotes station j and the ejector primary jet, see Fig. 6
JF = denotes a jet-augmented-flapped wing
l = lower surface
Q = denotes a quantity associated with the unblown suction airfoil
QJ = denotes an interference quantity due to a tangentially-blown trailing jet sheet on a flat-plate suction airfoil at zero angle of attack
s = denotes the ejector secondary flow (except x_s)
u = upper surface
αJ = denotes an interference quantity due to a tangentially-blown trailing jet sheet on a flat plate at angle of attack; includes the jet-reaction contribution when applied to force and moment coefficients
$\delta_f J$ = denotes an interference quantity due to a tangentially-blown trailing jet sheet on a flapped airfoil at zero angle of attack and flap deflection, δ_f; includes the jet-reaction contribution when applied to force and moment coefficients
α = due to α (not a partial derivative)
δ_f = due to δ_f (not a partial derivative)
∞ = denotes a freestream quantity
$\hat{}$ = denotes quantities associated with isentropic flow from P_j to p
$\tilde{}$ = denotes a velocity normalized by dividing by $\hat{U}_j$
$\bar{}$ = denotes a mean quantity

Introduction

WITHIN the last two decades considerable numbers of high-lift concepts for V/STOL aircraft have been proposed. One among these is the ejector-flapped wing (Fig. 1) also known as the augmentor wing, the ejector wing, the augmented jet-flap wing, etc. The ejector-flapped wing operates on a principle similar to the ordinary jet-flapped wing in that use is made of a trailing jet sheet to increase the circulation about the wing itself. It differs from the jet-flapped wing in the presence of ejector air intakes and the existence of an augmented trailing-edge momentum flux resulting from the ejector action. Since the augmented trailing-edge momentum flux is an internal-flow phenomenon, the basic difference in the external aerodynamics of the two systems is due to the air-intake flows. The intake flows behave as sink flows and are not accounted for in the usual jet-flap theory.[1,2]

Chan[3,4] has performed a theoretical analysis of an ejector-flapped wing based on a linearized thin-airfoil mathematical model which takes into account the intake sink flows. This paper treats the same theoretical model as does Chan, but by means of a different mathematical-numerical technique. The differences in the methodologies are briefly described in Ref. 5. As a consequence of a formulation in terms of permanently recorded Fourier coefficients, the present method is more versatile and more easily applied to the determination of distributed aerodynamic characteristics (surface pressures, local loads, and jet-sheet shape) than is the method of Chan. This paper also considers flap-hinge moments, whereas Chan does not. Additionally, the ejector flow characteristics are analyzed and the interfacing of the ejector internal flow with the external flow is studied. For comparable aerodynamic properties, the numerical results obtained by the two methods generally are in good agreement.

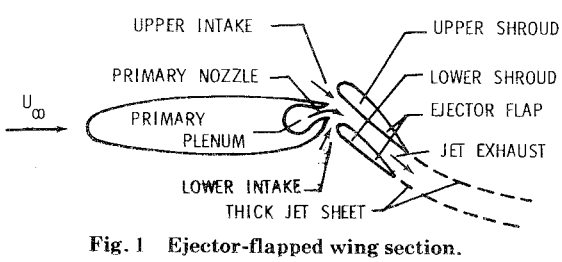

Fig. 1 Ejector-flapped wing section.

Analysis

Total Aerodynamics

A thin-airfoil representation of an ejector-flapped wing section having an upper intake only is shown in Fig. 2. The main airfoil and flap are approximated by straight lines, the ejector net intake flow by a surface sink† (not necessarily at the flap knee, but usually taken there), and the actual jet sheet of finite thickness by an infinitesimally thin sheet having a finite internal momentum. In this approximation the ejector intake and exhaust openings are required to be small relative to the airfoil chord. The internal and external flowfields are not required to match in fine detail at their interface, but the values of the ejector intake net mass flow and ejector exhaust total momentum flux must match those used in external flow aerodynamics.

Although Fig. 2 is illustrative of an ejector flap with an upper intake only, the solution obtained in this paper is valid for any sink (or source) location on the wing upper or lower surface. Since flow solutions are additive in the linearized treatment, a solution for an ejector flap having both upper and lower surface intakes is obtained by adding the individual solutions for upper and lower surface sinks. Additionally, solutions are additive for a series of sinks at different chordwise positions.

This paper is concerned only with "regular blowing," that is, blowing in which the jet leaves the trailing edge tangentially, as distinguished from "singular blowing," in which the jet leaves the trailing edge at an angle τ. In view of the linearity of solutions, Spence's[1] singular-blowing solution may be added to the present one if required.

The flow of Fig. 2 consists of three additive components: 1) the flow about a flat plate at angle of attack with regular blowing; 2) the flow about a flapped airfoil at zero angle of attack with regular blowing; 3) the flow about a flat-plate suction airfoil at zero angle of attack with regular blowing, as illustrated in Fig. 3. Note that the term "flat-plate suction airfoil" refers to a flat plate with a surface sink, i.e., a sink flow asymmetric to the x axis. Spence[1,2] solved the flows of Items 1 and 2. Item 3 is solved in this paper. The solution is accomplished by considering the given flow to consist of the sum of a known flow about an unblown flat-plate suction airfoil at zero angle of attack and an unknown interference flow associated with the trailing-edge blowing. The interference-flow solution is obtained by means of an adaptation of Spence's method.

The principal aerodynamic characteristics of the ejector-flapped wing are summarized by

$$u' = (u'_\alpha + u'_{\alpha J}) + (u'_{\delta_f} + u'_{\delta_f J}) + u'_Q + u'_{QJ} \quad (1)$$

$$\left.\begin{aligned} \gamma^{(\alpha)} &= (\gamma_\alpha{}^{(\alpha)} + \gamma_{\alpha J}{}^{(\alpha)}) + (\gamma_{\delta_f}{}^{(\alpha)} + \gamma_{\delta_f J}{}^{(\alpha)}) \\ &\quad + (\gamma_Q{}^{(\alpha)} + \gamma_{QJ}{}^{(\alpha)}) \\ \gamma^{(J)} &= \gamma_{\alpha J}{}^{(J)} + \gamma_{\delta_f J}{}^{(J)} + \gamma_{QJ}{}^{(J)} \end{aligned}\right\} \quad (2)$$

$$y^{(J)} = (y_\alpha{}^{(T)} + y_{\alpha J}{}^{(J)}) + (y_{\delta_f}{}^{(T)} + y_{\delta_f J}{}^{(J)}) + (y_Q{}^{(T)} + y_{QJ}{}^{(J)}) \quad (3)$$

$$c_\ell = (\partial c_\ell/\partial\alpha)\alpha + (\partial c_\ell/\partial\delta_f)\delta_f + (\partial c_\ell/\partial c_Q)c_Q \quad (4)$$

$$c_{m_o} = (\partial c_{m_o}/\partial\alpha)\alpha + (\partial c_{m_o}/\partial\delta_f)\delta_f + (\partial c_{m_o}/\partial c_Q)c_Q \quad (5)$$

$$c_{nf} = (\partial c_{nf}/\partial\alpha)\alpha + (\partial c_{nf}/\partial\delta_f)\delta_f + (\partial c_{nf}/\partial c_Q)c_Q \quad (6)$$

$$c_h = (\partial c_h/\partial\alpha)\alpha + (\partial c_h/\partial\delta_f)\delta_f + (\partial c_h/\partial c_Q)c_Q \quad (7)$$

$$c_T = c_J - 2(c_Q + \bar{h}_s/c) \quad (8)$$

†A sink for which the flow enters a point from only one side of a surface.

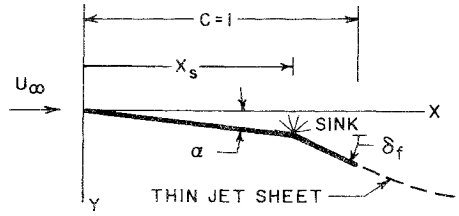

Fig. 2 Thin-airfoil representation of an ejector-flapped wing section with an upper-surface intake only.

where, if "a" represents any one of the coefficients, c_l, c_{m_o}, c_{nf}, and c_h, and "t" represents any one of the parameters, α, δ_f, and c_Q, in Eqs. (4–7) we may write

$$(\partial a/\partial t) = (\partial a/\partial t)_t + (\partial a/\partial t)_{tJ} \tag{9}$$

In Eqs. (1–3) and (9), a single subscript denotes that the affected quantity is due to variations in the subscript parameter without trailing-edge blowing. The double subscript (containing J and its antecedent) denotes the interference contribution of the affected quantity due to trailing-edge blowing and variations in the parameter antecedent to J. When applied to force and moment coefficients, a double subscripted term includes the jet-reaction contribution. The determination of the quantities subscripted with Q or QJ are the subject of this paper. The remaining quantities in Eqs. (1–8) generally are available in the technical literature. For details, see Ref. 5.

Flat-Plate Suction Airfoil Without Blowing

The problem under consideration in this section is the zero-angle-of-attack flow about an unblown flat plate with a surface sink on its upper surface, as would be illustrated by Fig. 3 if the jet sheet were absent. The problem is solved by conformally mapping the flow about a circular cylinder into that about a flat plate. In the circle plane, the flow consists of a uniform stream flowing past a circular cylinder with circulation, a sink on its surface, and a source of half the sink strength at the circle's center. The circulation is specified by enforcing the Kutta condition at the trailing edge of the flat plate.

From the potential flow equations[6] for the aforementioned flow, it can be shown that the perturbation velocity distributions on the surfaces of the flat plate are given by

$$\frac{u'_Q}{U_\infty} = \frac{\pm\,\sigma c_Q}{2\pi|x(1-x)|^{1/2}}\left\{\left(\frac{x_s}{1-x_s}\right)^{1/2} - \left[\sigma\left(\frac{x_s}{1-x_s}\right)^{1/2} \times \left(\frac{x}{1-x}\right)^{1/2} \pm 1\right]\left[\sigma\left(\frac{x}{1-x}\right)^{1/2} \mp \left(\frac{x_s}{1-x_s}\right)^{1/2}\right]^{-1}\right\} \tag{10}$$

where x_s denotes the chordwise sink location on a flat plate of unit chord. The parameter σ is assigned a value of 1 for a sink on the upper surface, and a value of -1 for a sink on the lower surface, and the upper and lower signs apply, respectively, for points on the upper and lower surfaces. The suction-flow coefficient c_Q is positive for a sink flow and is based on the total volumetric flow into the sink on the flat plate surface.

The vorticity is defined by $\gamma = (u'_u - u'_l)$. Substituting

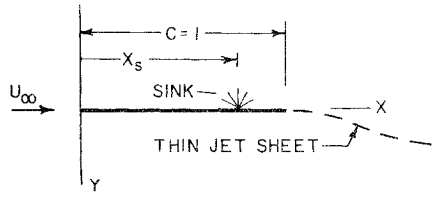

Fig. 3 Flat-plate suction airfoil with trailing-edge regular blowing.

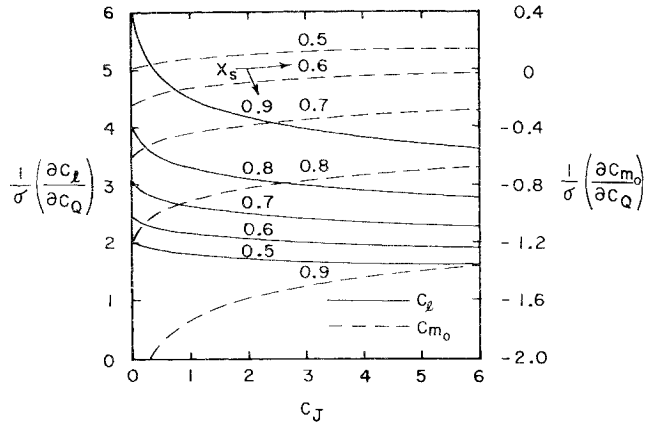

Fig. 4 Lift and pitching-moment characteristics of a flat-plate suction airfoil with trailing-edge regular blowing.

Eq. (10) in the vorticity relation yields the following for the vorticity distribution along the flat plate

$$\gamma_Q^{(a)}/U_\infty = \sigma(c_Q/\pi)\left[(x_s/1-x_s)^{1/2}\left(\frac{1-x}{x}\right)^{1/2}\right](x_s-x)^{-1} \tag{11}$$

It is important to note from Eq. (10) that $(u'_l)_Q \neq -(u'_u)_Q$. Therefore, $u'_Q \neq \gamma_Q/2$, and if airfoil surface pressure distributions are required, Eq. (10) and not Eq. (11), must be used for this purpose.

In principle, the vorticity distribution for an arbitrary sink distribution, $c_Q(x_s)$, over a finite region of the airfoil can be obtained by integrating Eq. (11) with respect[5] to x_s.

The lift coefficient and the nose-up pitching-moment coefficient about the leading edge are given, respectively, by

$$c_{\ell_Q} = 2\int_0^1 (\gamma_Q^{(a)}/U_\infty)dx \tag{12}$$

$$(c_{m_o})_Q = -2\int_0^1 x(\gamma_Q^{(a)}/U_\infty)dx \tag{13}$$

Substituting Eq. (11) in Eqs. (12) and (13), integrating, and taking the partial derivative with respect to c_Q yields

$$(\partial c_\ell/\partial c_Q)_Q = 2\sigma[x_s/(1-x_s)]^{1/2} \tag{14}$$

$$(\partial c_{m_o}/\partial c_Q)_Q = -\sigma(2x_s-1)[x_s/(1-x_s)]^{1/2} \tag{15}$$

If it is assumed that the intake sink is located at the flap-hinge point, the suction-airfoil contributions to the flap normal force and hinge moment are given by

$$(c_{nf})_Q = 2(c/c_f)\int_{x_s}^1 (\gamma_Q^{(a)}/U_\infty)dx \tag{16}$$

$$(c_h)_Q = -2(c/c_f)^2\int_{x_s}^1 (x-x_s)(\gamma_Q^{(a)}/U_\infty)dx \tag{17}$$

Substitution of Eq. (11) in Eq. (16) yields a divergent integral for $(c_{nf})_Q$. Hence, the present method fails for this property. A rough approximation to $(c_{nf})_Q$ can be obtained by replacing the lower limit on the integral by $x_s + (\bar{h}_i/2)$, where $\bar{h}_i$ is the mean height of the injector inlet.

Substituting Eq. (11) in Eq. (17), integrating, and taking the partial derivative with respect to c_Q yields

$$(\partial c_h/\partial c_Q)_Q = \sigma(2/\pi)(c/c_f)^2\{-x_s + \tfrac{1}{2}[x_s/(1-x_s)]^{1/2}\cos^{-1}(2x_s-1)\} \tag{18}$$

Replacing $w(x)$ by $U_\infty y'(x)$ in the downwash equation yields the following expression from which the trailing streamline shape may be determined

$$dy/dx = -(1/2\pi U_\infty)\int_0^1 \gamma_Q{}^{(a)}(\xi)d\xi/(\xi - x) \quad (19)$$

Substituting Eq. (11) in Eq. (19), integrating with respect to ξ for $x > 1$ with the aid of Spence's[1] Eqs. (57) and (66), and finally integrating with respect to x, yields the following result for the shape of the trailing streamline

$$y_Q{}^{(T)}/c_Q = (\sigma/2\pi)[x_s/(1 - x_s)]^{1/2}F(x, x_s) \quad (20)$$

where

$$F(x, x_s) \equiv -(\pi/2)(x_s - x_s{}^2)^{1/2} + \tfrac{1}{2}(2x_s - 1)\ell n|2(x^2 - x)^{1/2} + 2x - 1| + \ell n|(x - 1)^{1/2} + x^{1/2}| - (x_s - x_s{}^2)^{1/2}\sin^{-1}[(2xx_s - x - x_s)/|x - x_s|] \quad (21)$$

Equation (20) is numerically in agreement with Chan's result (Fig. 13 of Ref. 4) for $c_J = 0$ and $x_s = 0.7$.

Flat-Plate Suction Airfoil at Zero Angle of Attack with Regular Blowing

The flow problem is illustrated in Fig. 3. The governing equations are Eqs. (50) and (51) in Spence.[1] These equations are a pair of coupled integro-differential equations involving the vorticity distributions on the airfoil and jet sheet and the airfoil and jet-sheet slopes. In Spence's[1] applications, the nondimensional vorticity distribution, $f(x)$, on the airfoil is "a priori" unknown. In the present application, $f(x)$ is the sum of an unknown distribution and the known distribution for the unblown flat-plate suction airfoil. It is convenient to write

$$f(x) = f_Q(x) + f_{QJ}(x) \quad (22)$$

where $f_{QJ}(x)$ is the unknown vorticity distribution induced on the plate by the jet sheet in the presence of the unblown suction airfoil, and $f_Q(x)$ is the known distribution given by Eq. (11). Noting that $\epsilon(x) = 0$ in the present problem, substituting Eq. (22), with $f_Q(x)$ replaced by Eq. (11), into Spence's[1] Eqs. (50) and (51), and evaluating the appropriate integrals by means of Eqs. (65) and (66) in Spence's[1] paper yields the following

$$\int_0^1 \frac{f_{QJ}(x)}{\xi - x}d\xi + \int_1^\infty \frac{g'(\xi)}{\xi - x}d\xi = 0 \qquad (0 < x < 1) \quad (23)$$

$$\int_0^1 \frac{f_{QJ}(x)}{\xi - x}d\xi + \int_1^\infty \frac{g'(\xi)}{\xi - x}d\xi = \pi\lambda g(x) - \sigma c_Q\left(\frac{x_s}{1 - x_s}\right)^{1/2}\left(\frac{x - 1}{x}\right)^{1/2}(x_s - x)^{-1} \qquad (x > 1) \quad (24)$$

where $g(x) = -(\frac{1}{2})c_J y'(x)$, and the boundary conditions are $g(1) = g(\infty) = 0$.

Equations (23) and (24) are of the same general form as Spence's Eqs. (50) and (51), with $\epsilon(x)$ set equal to zero. The methods used by Spence[1] to reduce his pair of equations to a single integro-differential equation, and to solve for the interference vorticity distribution along the airfoil, therefore, also may be applied to Eqs. (23) and (24). Replacing $g(x)$ by $2c_Q G(x)$ and applying the procedure outlined on pp. 53 and 54 of Ref. 1 to Eqs. (23) and (24) yields the following integro-differential equation for the unknown vorticity distribution, $G(x)$, on the trailing jet sheet

$$\left(\frac{x - 1}{x}\right)^{1/2}\int_1^\infty \left(\frac{\eta}{\eta - 1}\right)^{1/2}\frac{G'(\eta)d\eta}{\eta - x} - \pi\lambda G(x) = -\frac{\sigma}{2}\left(\frac{x_s}{1 - x_s}\right)^{1/2}\left(\frac{x - 1}{x}\right)^{1/2}(x_s - x)^{-1} \quad (25)$$

with $x > 1$ and $G(1) = G(\infty) = 0$. Also, by the methods of pp. 53 and 54 of Ref. 1, it may be shown that

$$\gamma_{QJ}{}^{(a)}(x)/U_\infty = \frac{2\sigma c_Q}{\pi}\left(\frac{1 - x}{x}\right)^{1/2}\int_1^\infty \left(\frac{\eta}{\eta - 1}\right)^{1/2}\frac{G'(\eta)d\eta}{\eta - x} \quad (26)$$

where $G'(\eta)$ is obtained from the solution of Eq. (25).

Equation (25) may be conveniently transformed by the substitutions

$$x = \cos^{-2}(\varphi/2), \quad \eta = \cos^{-2}(\theta/2) \quad (27)$$

The function $G'(\varphi)$, where $G'(\varphi) \equiv dG(\varphi)/d\varphi$, is now expanded in the Fourier series

$$G'(\varphi) = \sin(\varphi/2)\sum_{n=0}^{\infty} E_n \cos n\varphi \quad (28)$$

in the range $0 \le \varphi \le \pi$. The corresponding series for $G(\varphi)$ is

$$G(\varphi) = \sum_{n=0}^{\infty} E_n(2\cos\tfrac{1}{2}\varphi\cos n\varphi + 4n\sin\tfrac{1}{2}\varphi\sin n\varphi)/(4n^2 - 1) \quad (29)$$

Changing variables in Eq. (25), substituting Eqs. (28) and (29) in the result, and evaluating the resulting integrals with the aid of Spence's Eqs. (87) and (88) yields the following

$$E_0\sin\varphi + \sum_{n=1}^{\infty} E_n(1 + \cos\varphi)\sin n\varphi + 2\lambda G(\varphi)/\cos\tfrac{1}{2}\varphi = (\sigma/\pi)[x_s/(1 - x_s)]^{1/2}\sin\varphi/[x_s(1 + \cos\varphi) - 2] \quad (30)$$

where $G(\varphi)$ is given by Eq. (29).

Equation (30) is solved by satisfying it at N pivotal points yielding N simultaneous equations. The pivotal points are determined by

$$\varphi_m = m\pi/N, \quad m = 0, 1, 2, \ldots N - 1 \quad (31)$$

Equation (30) then yields

$$\sum_{n=0}^{\infty}(a_{mn} + \lambda b_{mn})E_n = e_m \quad (32)$$

where

$$a_{mo} = \sin\varphi_m \qquad (n = 0) \quad (33)$$

$$a_{mn} = (1 + \cos\varphi_m)\sin n\varphi_m \qquad (n > 0) \quad (34)$$

$$b_{mn} = 4(\cos n\varphi_m + 2n\tan\tfrac{1}{2}\varphi\sin n\varphi_m)/(4n^2 - 1) \quad (35)$$

$$e_m = (\sigma/\pi)[x_s/(1 - x_s)]^{1/2}\sin\varphi_m/[x_s(1 + \cos\varphi_m) - 2] \quad (36)$$

The coefficients listed in Eqs. (33–36) were calculated to 15 decimal places for $N = 9$, $x_s = 0.5$, 0.6, 0.7, 0.8, and 0.9, and $\sigma = 1$. The sets of nine simultaneous equations resulting from the foregoing values of x_s and for values of c_J equal to 0.25, 0.5, 1.0, 2.0, 4.0, and 6.0 were solved on a CDC 6600 digital computer. The values of E_n so obtained are recorded in Table 1.

Transforming Eq. (26) to the φ and θ variables according to Eqs. (27), substituting Eq. (28) in the resulting integrand, integrating with the help of Spence's[1] Eqs. (87) and (88), and finally transforming back to the x variable yields the following for the interference vorticity distribution along the airfoil

$$\gamma_{QJ}{}^{(a)}/U_\infty = 2\sigma c_Q[2E_0X/(1 + X) + \sum_{n=1}^{N-1} E_n X^n]x^{-3/2} \quad (37)$$

where $X \equiv X(x)$ as given in the nomenclature. The corresponding surface perturbation velocities are given by

$$u'_{QJ} = \pm\gamma_{QJ}{}^{(a)}/2 \quad (38)$$

where the upper sign applies to the upper surface and the lower sign to the lower surface. Other aerodynamic properties may be obtained by noting that the mathematics is analogous to that of Spence[1] for regular blowing with c_Q replacing α and E_n replacing B_n. Hence, by comparison

Table 1 Fourier coefficients for a flat-plate suction airfoil with trailing-edge regular blowing ($\sigma = 1$)

		E_n					
x_s	n	$c_J = 0.25$	$c_J = 0.50$	$c_J = 1$	$c_J = 2$	$c_J = 4$	$c_J = 6$
0.5	0	−0.0075	−0.0114	−0.0163	−0.0222	−0.0288	−0.0327
	1	−0.0186	−0.0290	−0.0430	−0.0605	−0.0808	−0.0935
	2	−0.0147	−0.0209	−0.0268	−0.0305	−0.0295	−0.0259
	3	−0.0069	−0.0071	−0.0049	+0.0003	+0.0071	+0.0105
	4	−0.0040	−0.0037	−0.0029	−0.0031	−0.0058	−0.0086
	5	−0.0020	−0.0014	−0.0007	+0.0001	+0.0019	+0.0039
	6	−0.0013	−0.0010	−0.0008	−0.0008	−0.0013	−0.0023
	7	−0.0007	−0.0004	−0.0001	+0.0001	+0.0005	+0.0010
	8	−0.0003	−0.0003	−0.0002	−0.0002	−0.0003	−0.0005
0.6	0	−0.0108	−0.0162	−0.0230	−0.0310	−0.0396	−0.0447
	1	−0.0266	−0.0410	−0.0599	−0.0832	−0.1096	−0.1259
	2	−0.0220	−0.0311	−0.0400	−0.0461	−0.0461	−0.0423
	3	−0.0112	−0.0122	−0.0098	−0.0033	+0.0054	+0.0099
	4	−0.0064	−0.0061	−0.0048	−0.0046	−0.0076	−0.0110
	5	−0.0033	−0.0024	−0.0013	−0.0002	+0.0018	+0.0042
	6	−0.0020	−0.0016	−0.0012	−0.0011	−0.0016	−0.0027
	7	−0.0010	−0.0006	−0.0002	+0.0001	+0.0005	+0.0011
	8	−0.0005	−0.0004	−0.0003	−0.0003	−0.0004	−0.0006
0.7	0	−0.0166	−0.0244	−0.0341	−0.0452	−0.0568	−0.0635
	1	−0.0402	−0.0608	−0.0874	−0.1193	−0.1546	−0.1760
	2	−0.0348	−0.0490	−0.0631	−0.0732	−0.0753	−0.0716
	3	−0.0197	−0.0223	−0.0203	−0.0126	−0.0013	+0.0048
	4	−0.0114	−0.0112	−0.0094	−0.0085	−0.0116	−0.0155
	5	−0.0060	−0.0048	−0.0030	−0.0015	+0.0011	+0.0039
	6	−0.0036	−0.0028	−0.0021	−0.0018	−0.0022	−0.0034
	7	−0.0018	−0.0012	−0.0006	−0.0001	+0.0005	+0.0012
	8	−0.0009	−0.0006	−0.0005	−0.0004	−0.0005	−0.0007
0.8	0	−0.0285	−0.0411	−0.0561	−0.0724	−0.0891	−0.0985
	1	−0.0678	−0.1002	−0.1405	−0.1869	−0.2368	−0.2662
	2	−0.0621	−0.0865	−0.1106	−0.1290	−0.1359	−0.1330
	3	−0.0396	−0.0468	−0.0469	−0.0382	−0.0236	−0.0153
	4	−0.0244	−0.0253	−0.0228	−0.0208	−0.0238	−0.0284
	5	−0.0136	−0.0119	−0.0091	−0.0066	−0.0033	+0.0003
	6	−0.0079	−0.0065	−0.0051	−0.0043	−0.0045	−0.0058
	7	−0.0041	−0.0029	−0.0018	−0.0010	−0.0002	+0.0006
	8	−0.0019	−0.0014	−0.0010	−0.0009	−0.0009	−0.0011
0.9	0	−0.0651	−0.0903	−0.1181	−0.1468	−0.1743	−0.1893
	1	−0.1503	−0.2130	−0.2858	−0.3647	−0.4449	−0.4904
	2	−0.1471	−0.1997	−0.2508	−0.2908	−0.3110	−0.3116
	3	−0.1102	−0.1337	−0.1440	−0.1376	−0.1194	−0.1077
	4	−0.0767	−0.0845	−0.0839	−0.0808	−0.0835	−0.0892
	5	−0.0487	−0.0484	−0.0442	−0.0398	−0.0349	−0.0300
	6	−0.0301	−0.0281	−0.0250	−0.0230	−0.0224	−0.0237
	7	−0.0168	−0.0145	−0.0121	−0.0102	−0.0089	−0.0078
	8	−0.0077	−0.0066	−0.0055	−0.0050	−0.0048	−0.0049

with Spence,[1]

$$y_{QJ}^{(T)}/\sigma c_Q = 2E_0\left|\ell n \tan\left(\tfrac{1}{4}\varphi + \tfrac{1}{4}\pi\right) - \sin\tfrac{1}{2}\varphi\right| + \sum_{n=1}^{N-1} 2E_n(\cos\tfrac{1}{2}\varphi \sin n\varphi - 2n \sin\tfrac{1}{2}\varphi \cos n\varphi)/(4n^2 - 1) \quad (39)$$

$$\gamma_{QJ}^{(J)}/U_\infty = 2\sigma c_Q \cos^3\tfrac{1}{2}\varphi \sum_{n=0}^{N-1} E_n \cos n\varphi \quad (40)$$

$$(\partial c_\ell/\partial c_Q)_{QJ} = \sigma 4\pi E_0 \quad (41)$$

$$(\partial c_{m_o}/\partial c_Q)_{QJ} = -\sigma \sum_{n=0}^{N-1} E_n I_n^{(1)}(0) \quad (42)$$

where

$$I_0^{(m)}(\nu) \equiv 8\int_\nu^1 \frac{x^m x^{-3/2} X dx}{1 + X} \quad (m = 0, 1; n = 0) \quad (43)$$

$$I_n^{(m)}(\nu) \equiv 4\int_\nu^1 x^m x^{-3/2} X^n dx \quad (m = 0, 1; n = 1, 2 \ldots) \quad (44)$$

Spence[1] comments that the integrals $I_n^{(1)}(0)$ can be evaluated by recursion formulas. He does not supply the analytic results, but does provide numerical values through $n = 8$. Hayashi[7] provides analytic relations for the more general integral $I_n^{(m)}(\nu)$ (identified differently by Hayashi) which is required in determining the flap normal-force and hinge-moment coefficients.

If, as for the unblown airfoil, we assume that the intake is located at the flap-hinge point, the interference contribution to the flap normal-force and hinge-moment coefficients are defined by Eqs. (16) and (17) with the "Q" subscripted quantities replaced by "QJ" subscripted quantities. Substitution of Eq. (37) in the resulting relations yields

$$(\partial c_{nf}/\partial c_Q)_{QJ} = \sigma(c/c_f) \sum_{n=0}^{N-1} E_n I_n^{(0)}(x_s) \quad (45)$$

$$(\partial c_h/\partial c_Q)_{QJ} = -\sigma(c/c_f)^2 \sum_{n=0}^{N-1} E_n[I_n^{(1)}(x_s) - x_s I_n^{(0)}(x_s)] \quad (46)$$

Analogous relations for the flap normal-force and hinge-moment coefficients are not available from Spence[2] since he does not treat these analytically, but provides selected numeric results only. A specific aerodynamic characteristic for the flat-plate suction airfoil at zero angle of attack with regular blowing is the sum of the unblown characteristic denoted by the subscript Q and the interference characteristic denoted by the subscript QJ.

Curves showing $(\partial c_l/\partial c_Q)/\sigma$ and $(\partial c_{m_o}/\partial c_Q)/\sigma$ as a

function of c_J for several sink locations are presented in Fig. 4. Similar curves are presented by Chan.[3] The differences in magnitudes as calculated by Chan and the present author generally are less than about 5%. It is observed in Fig. 4 that the sink effect becomes stronger as the sink approaches the trailing edge, a well-known property of suction airfoils. It is seen also that for a sink on the upper surface, the interference effect of the jet sheet decreases the lift coefficient and increases the nose-up pitching-momentum coefficient.

If, for an ejector-flapped airfoil with an upper surface intake only, the curves of $(\partial c_l/\partial c_Q)$ in Fig. 4 are compared with the jet-augmented flap-effectiveness curves, $(\partial c_l/\partial \delta_f)$, of Ref. 2 on the basis that c_Q and δ_f are of the same order of magnitude, it can be seen (as noted by Chan[3]) that the suction-effect contribution to the lift is quite appreciable. For a 30% flap and $c_J = 1$, for example, the suction-effect contribution to the lift is approximately 40% of that due to the basic jet-augmented flap. It is one of the purposes of this paper to estimate c_Q by means of idealized ejector-flow relations and thereby determine in more detail those conditions under which the suction-effect contribution to the lift is significant.

Suction Coefficient

The analysis thus far has been concerned with a thin-airfoil approximation in which the real airfoil and the ejector shroud (or shrouds) are taken to lie on a single skeletal line. A real ejector-flapped wing, however, has a finite-height intake (or intakes) and a question arises regarding the application of a limiting process in which the intake height is reduced to zero in a manner such that the thin-airfoil aerodynamics most appropriately represents the real-airfoil aerodynamics. Since the thin-airfoil approximation is an imperfect representation of the real flow, there cannot be a one-to-one correspondence between the real and theoretical flows, and a decision must be made regarding which properties are to be matched in a thin-airfoil representation. Certainly the lift coefficient is an important quantity to be conserved. The thrust coefficient is of lesser importance in the thin-airfoil representation since it is easily determined from considerations of conservation of global momentum applied directly to the real flow. As an intermediate step to taking the limiting process, consider the "idealized real wing" shown in Fig. 5 representing a real ejector-flapped wing (with upper shroud only) at zero angle of attack and zero flap deflection. In this representation, the main airfoil and the shroud are of infinitesimal thickness, but the total airfoil is not a thin airfoil because of the small, but finite, intake height (exaggerated in the figure for clarity). For an arbitrary intake flow in Fig. 5, there is no formal procedure for applying a limiting process in which the lift coefficient is held constant. However, as will be shown subsequently, the appropriate limit can be obtained by inductive reasoning. On the other hand, the limit in which the intake mass flow is held constant while the intake height is reduced to zero is easily implemented by simply taking the theoretical sink mass flow equal to the gross intake mass flow of the real wing. In this case, the suction coefficient used in the theoretical relations is the ejector gross suction coefficient, $\check{c}_Q$. Use of the gross suction coefficient is advocated by Chan[4,8] and by Lopez and Halsey[9] of Douglas Aircraft Company. The present writer advocates the use of the ejector net suction coefficient, c_Q, since it is shown below that, for a particular case, the use of the gross suction coefficient fails to yield the proper lift coefficient. For purposes of the present argument, the idealized real flow in Fig. 5 is taken to be the real flow since the intake has a finite height. Now consider a flow in which the intake capture streamline is parallel to the main airfoil as shown by the dashed line $a'b$ in Fig. 5. For this situation,

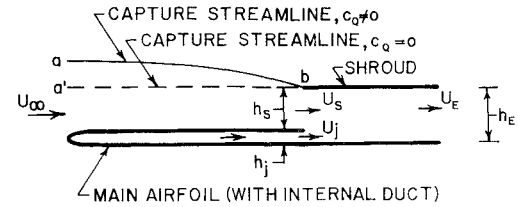

Fig. 5 Idealized ejector-flapped wing section defining $c_Q = 0$.

$c_Q = 0$ and $\check{c}_Q = h_s/c$. Since in this case all the streamlines of the idealized real flow are parallel, there is no lift (or moment) on the real wing, hence the thin-airfoil theory should yield zero lift and moment. Use of the ejector net suction coefficient, $c_Q = 0$, in the thin-airfoil results of Fig. 4 for this case, yields the proper zero lift and moment; use of the ejector gross suction coefficient, $\check{c}_Q = h_s/c$, however, yields incorrect nonzero values for the lift and moment. It follows that the thin-airfoil lift and moment coefficients based on $\check{c}_Q$ will be in error also for an arbitrary intake mass flow ($\check{c}_Q \neq h_s/c$). The foregoing differences are discussed from a slightly different viewpoint in Ref. 5.

Although matching of the thin-airfoil and real flows by means of the net suction coefficient yields the proper lift and pitching-moment coefficients in the thin-airfoil approximation, it fails to give the correct thrust coefficient. This latter property [see Eq. (8)], as previously noted, is easily obtained from the real flow. Inconsistencies of this type are characteristic of approximate representations of complicated flows,‡ and are tolerated for the purposes of obtaining an engineering estimate of the problem being solved. It is believed that the foregoing arguments support the contention that the ejector net suction coefficient, c_Q, is the proper coefficient to use in the thin-airfoil approximation.

One-Dimensional Ejector-Flow Relations

A schematic representation of an ejector flap is given in Fig. 6. The ejector internal flow is taken to be incompressible and is analyzed on the basis of assumptions that the flow properties are uniform at any given cross-sectional station and there are no flow losses except those due to mixing. It is recognized that this is an oversimplification for aircraft design purposes. The purpose here, however, is to delineate the general characteristics of the integrated external-internal aerodynamic system, and this is best accomplished by keeping the mathematical modeling as simple as possible.

The primary air is injected at station j (see Fig. 6), and

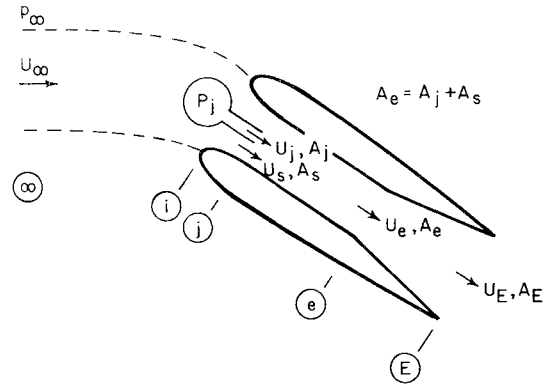

Fig. 6 Schematic representation of an ejector flap.

‡In Spence's[1] jet-flap theory, for example, the trailing jet sheet contains a finite momentum flux and zero mass flux.

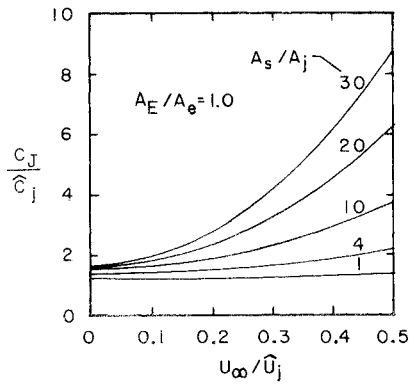

Fig. 7 Exit-momentum augmentation ratio as a function of the forward-speed ratio and injection-area ratio.

mixing with the secondary air is assumed to be completed at the end of the constant cross-sectional area region extending between stations j and e. It is assumed also that the static pressures of the primary and secondary streams are equal at the injection station j and that the diffuser-exit static pressure is equal to the freestream static pressure. In view of the assumption of loss-free flow in the intake, the primary nozzle, and the diffuser, Bernoulli's equation is applicable to these regions.

In the ejector analytics, flow velocities are nondimensionalized by dividing by $\hat{U}_j$, where $\hat{U}_j$ is the velocity attained by the primary nozzle exhausting isentropically to the freestream static pressure. This velocity is a measure of the primary-air total pressure, the quantity most likely to be held constant during the major portion of a landing or takeoff operation.

On the basis of the aforementioned assumptions, the governing equations for the ejector internal flow are

$$2\tilde{U}_j^2 - \tilde{U}_s^2(1-\Omega_j) - \tilde{U}_E^2(1+\Omega_D^2)(1+\Omega_j) + \tilde{U}_\infty^2(1+\Omega_j) = 0 \quad (47)$$

$$\tilde{U}_j + \tilde{U}_s\Omega_j = \tilde{U}_E(1+\Omega_j)\Omega_D \quad (48)$$

$$\tilde{U}_j^2 = \tilde{U}_s^2 - \tilde{U}_\infty^2 + 1 \quad (49)$$

Equations (47) and (48) are respectively expressions of conservation of momentum and mass between stations "j" and "e" in Fig. 6. These forms of the conservation equations were derived from the basic forms by appropriate use of Bernoulli's equation, continuity, and the previously mentioned assumptions. Equation (49) is a consequence of the equality of p_s and p_j and the use of Bernoulli's equation for the primary and secondary flows.

The quantities $\tilde{U}_j$ and $\tilde{U}_E$ may be eliminated from Eq.

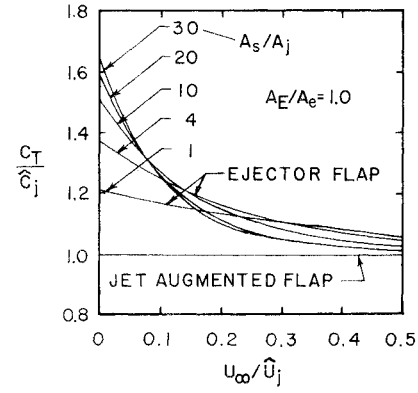

Fig. 8 Thrust-augmentation ratio as a function of the forward-speed ratio and injection-area ratio.

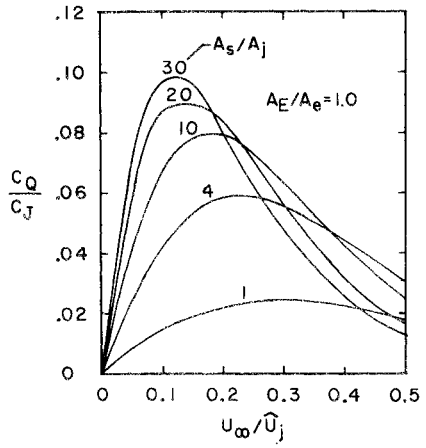

Fig. 9 Ratio of net suction coefficient to jet-momentum coefficient as a function of the forward-speed ratio and the injection-area ratio.

(47) through the use of Eqs. (48) and (49), yielding the following quadratic equation in $\tilde{U}_s^2$

$$a_o\tilde{U}_s^4 + (b_o + b_2\tilde{U}_\infty^2)\tilde{U}_s^2 + c_o + c_2\tilde{U}_\infty^2 + c_4\tilde{U}_\infty^4 = 0 \quad (50)$$

where

$$a_o = (\Omega_j+1)^2[\Omega_j^2 - 2(1+2\Omega_D^2)\Omega_j + 1] \quad (51)$$

$$b_o = -4\Omega_D^2\Omega_j^3 + 2(2\Omega_D^4 - 5\Omega_D^2 - 1)\Omega_j^2 + 4(\Omega_D^4 - 2\Omega_D^2)\Omega_j - 2\Omega_D^2 + 2 \quad (52)$$

$$b_2 = -2\Omega_D^2\Omega_j^4 + 4\Omega_D^4\Omega_j^3 + 2(2\Omega_D^4 + 3\Omega_D^2 + 1)\Omega_j^2 + 4\Omega_D^2\Omega_j - 2 \quad (53)$$

$$c_o = [\Omega_D^2 - (1-2\Omega_D^2\Omega_j)] \quad (54)$$

$$c_2 = 2(1+\Omega_D^2\Omega_j^2)[\Omega_D^2 - (1-2\Omega_D^2\Omega_j)] \quad (55)$$

$$c_4 = (1+\Omega_D^2\Omega_j^2)^2 \quad (56)$$

Equation (50) may be solved for $\tilde{U}_s^2$ by the standard quadratic formula. For the sign options preceding the radical, the negative sign must be selected. The numerics are much more convenient, however, if Eq. (50) is divided through by a_o and then solved by the quadratic formula. In this case, the sign of the radical is given by $(-\text{sgn } a_o)$.

Solution of Eq. (50) yields $\tilde{U}_s$ as a function of the forward-speed parameter $\tilde{U}_\infty$, the injection area ratio Ω_j, and the diffuser area ratio Ω_D. With $\tilde{U}_s$ known, $\tilde{U}_E$ and $\tilde{U}_j$ can be determined as functions of $\tilde{U}_\infty$, Ω_j, and Ω_D by means of Eqs. (48) and (49). By appropriate substitutions, the ejector coefficients, $\hat{c}_j$, c_j^*, c_J, $\hat{c}_t$, c_T, c_Q, and $\hat{c}_Q$ (see Nomenclature) also can be determined as functions of $\tilde{U}_\infty$, Ω_j, and Ω_D.

Some selected ejector characteristics as functions of the forward-speed ratio are shown in Figs. 7-9 for a diffuser area ratio of unity. For aircraft high-lift operations, forward-speed ratios in the vicinity of 0.1 are to be expected. This corresponds to a flight velocity of 100 fps and a primary nozzle velocity of 1000 fps.

Shown in Fig. 7 is the exit-momentum augmentation ratio $c_J/\hat{c}_J$. This parameter has a value of unity for a jet flap and is a measure of the increase in the exit-momentum coefficient of an ejector flap over that of a jet flap having the same primary-air supply pressure ratio. The parameter, $c_J/\hat{c}_j$ is important to the lift. It is apparent from the figure that both forward speed and increased injection-area ratio are beneficial to increasing this ratio. The thrust, however, behaves differently as may be seen

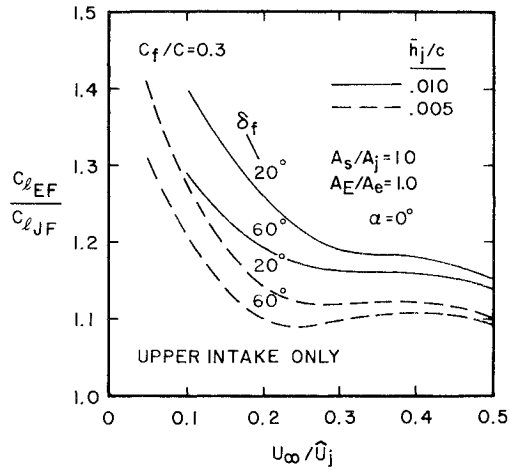

Fig. 10 Relative lift performance of ejector-flapped and jet-augmented-flapped wings.

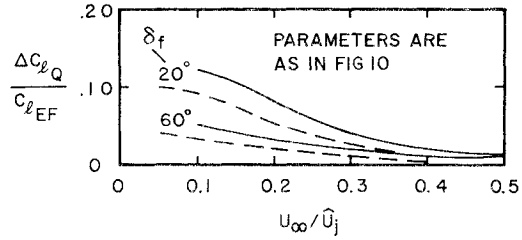

Fig. 11 Suction contribution to the lift of ejector-flapped wings.

in Fig. 8. It is seen that regardless of the injection-area ratio the thrust augmentation decreases with forward speed, reaching values less than 1.1 for speed ratios in excess of 0.3. At small forward-speed ratios the thrust augmentation increases with increasing injection-area ratio while at the high ratios the opposite occurs. In the region of potential interest for high-lift systems ($U_\infty/\hat{U}_j \cong 0.1$) the injection-area ratio has little effect, except at the very low area ratios.

Finally, the behavior of the net suction coefficient with forward speed is shown in Fig. 9. It is seen in this figure that the suction coefficient reaches a maximum value at a particular forward-speed ratio. The maximum suction coefficient and the corresponding speed ratio are seen to be a function of the injection-area ratio, although at the higher area ratios the dependence is rather weak. For area ratios of interest for high-lift systems ($A_s/A_j \cong 10$) the maximum coefficients occur at forward-speed ratios typical to high-lift systems. It is seen also from Fig. 9 that for the maximum suction coefficients and a c_J of unity, c_Q and δ_f are of the same order of magnitude for flap angles of approximately 5°.

Relative Lift Performance

The lift performance of an ejector-flapped wing relative to that of a wing with a jet-augmented flap, based on the relations given in this paper, is shown in Fig. 10 for typical values of the pertinent parameters. It can be seen in the figure that for forward-speed ratios below 0.3 the ejector-flap lift is substantially superior and continues to increase in superiority as the forward speed is reduced. The superiority also increases with increasing ejector size as indicated by the gains accompanying the change in the relative nozzle height from 0.005 to 0.010. The lift superiority of the ejector-flapped wing also increases with decreasing flap deflection. As may be seen in Fig. 11, this effect is due to the fact that the relative suction contribution to the lift of the ejector-flapped wing is larger at lower flap angles.

Conclusions

On the basis of simple mathematical models of the external and internal flows, an integrated theoretical analysis of the aerodynamics of an ejector-flapped wing has been presented. The external aerodynamics has been systemized for ease of application by inclusion of a table of Fourier coefficients. Incompressible, idealized, forward-speed ejector-flow equations have been presented in a normalized form believed to be most appropriate for interfacing with the external aerodynamics. Some parametric curves of ejector forward-speed characteristics have been presented. Although forward-speed effects on exit momentum and net thrust of ejectors are generally well-known, it is believed to have been worthwhile to re-emphasize these and cast them in a form appropriate for interfacing with the external aerodynamics. The delineation of the suction-flow coefficient characteristics is believed to be new or at least relatively unfamiliar. The idealized lift performance of an ejector-flapped wing relative to a jet-augmented flapped wing has been compared and the ejector flapped wing was found to be substantially superior at low forward-speed ratios. Finally, it was determined that the suction effect on the lift is most significant at low flap angles.

Despite the idealized character of the flow model, it is believed that it adequately delineates the important trends. Because of its relative simplicity, it is easily amenable to empirical modification for use as a preliminary design tool.

References

[1]Spence, D. A., "The Lift Coefficient of a Thin Jet-Flapped Wing," *Proceedings of the Royal Society of London*, Ser. A, Vol. 238, No. 1212; Dec. 1956, pp. 46-48.

[2]Spence, D. A., "The Lift on a Thin Aerofoil with a Jet-Augmented Flap," *The Aeronautical Quarterly*, Vol. 9, Pt. 3, Aug. 1958, pp. 287-299.

[3]Chan, Y. Y., "Lift Induced by Suction Flaps on Augmentor Wings," *Canadian Aeronautics and Space Institute Transactions*, Vol. 3, No. 2, Sept. 1970, pp. 107-110.

[4]Chan, Y. Y., "The Lift on a Two-Dimensional Augmentor Wing. National Research Council of Canada," Aeronautical Rep. LR-523, (AD 692 351), April 1969, National Aeronautical Establishment of Canada, Ottawa, Canada.

[5]Woolard, H. W., "Thin-Airfoil Theory of an Ejector-Flapped Wing Section," AIAA Paper 74-187, Washington, D.C., 1974.

[6]Wygnanski, I. and Newman, B. G., "The Effect of Jet Entrainment on Lift and Moment for a Thin Aerofoil with Blowing," *The Aeronautical Quarterly*, Vol. XV, Pt. 2, May 1964, pp. 122-159.

[7]Hayashi, T. T., "The Two-Dimensional Jet-Flap Theory," Report No. MDC J1089, Dec. 1971, Douglas Aircraft Company, Long Beach, Calif.

[8]Chan, Y. Y., National Aeronautical Establishment, Ottawa, Canada, private communication, June 1974.

[9]Lopez, M. L. and Halsey, N.D., Douglas Aircraft Co., Long Beach, Calif., private communication, June 1974.